Costa, CM.; Sabater I Serra, R.; Balado, AA.; Gómez Ribelles, JL.; Lanceros-Méndez, S. (2020). Dielectric relaxation dynamics in poly(vinylidene fluoride)/Pb(Zr0.53Ti0.47)O3 composites. Polymer. 204:1-9. https://doi.org/10.1016/j.polymer.2020.122811

Dielectric relaxation dynamics in poly(vinylidene fluoride) /$Pb(Zr_{0.53}Ti_{0.47})O_3$ composites

C. M. Costa[1], R. Sabater i Serra[2,3], A. Andrio Balado[4], J. L. Gómez Ribelles[2,3], S. Lanceros-Méndez[5,6]

[1]Centro de Física, Universidade do Minho, Campus de Gualtar, 4710-058 Braga, Portugal.

[2]Centre for Biomaterials and Tissue Engineering, CBIT, Universitat Politècnica de València, 46022, Valencia, Spain

[3]Biomedical Research Networking Center on Bioengineering, Biomaterials and Nanomedicine (CIBER-BBN), Valencia, Spain

[4]Departament de Física, Universidad Jaime I, 12071 Castellón, Spain

[5]BCMaterials, Basque Center for Materials, Applications and Nanostructures, UPV/EHU Science Park, 48940 Leioa, Spain

[6]IKERBASQUE, Basque Foundation for Science, 48013 Bilbao, Spain

Abstract: Polymer-ceramic composites based on poly(vinylidene fluoride) and ceramic particles of the inorganic piezoelectric material $Pb(Zr_{0.53}Ti_{0.47})O_3$ were prepared with different particle concentrations and size by solution casting in the non-polar (α–) and polar (β-) phases of the polymer. The influence of amount and particle size on the overall dielectric response of α- and β-phase matrix composites was analyzed, focusing on the dielectric relaxation processes. The cooperative segmental motions within the PVDF amorphous phase (low-temperature β-relaxation), are strongly affected by the inclusion of the fillers, both in the α– and β-phase matrix composites. The complex permittivity analyzed by the Havriliak-Negami equation model (NH) and the fragility parameter indicates that the PZT ceramic filler induces heterogeneity in the polymer matrix. For α-PVDF/PZT composites, the strength of the relaxation process increases with increasing

the filler amount and it is nearly independent on particle size. The behavior of the HN shape parameters, more noticeable for filler content of 20% or higher, shows that the relaxation dynamics is influenced by the polymer nucleation kinetics. PVDF/PZT composites in β-phase matrix exhibit a strong increase in the relaxation strength for PVDF/PZT composites with 40% of ceramic fillers, and the process becomes more symmetric when the amount of filler increases. The detected variations in the relaxation dynamics in both α- and β-phase matrix composites is strongly affected by the ceramic filler and the interface between the ceramic microparticles and the polymer.

Keywords: Composites; dielectric analysis; PVDF; PZT; Smart materials

1. Introduction

Polymer-ceramic composite properties are the result from the combination/mixture of two or more different materials, offering the possibility of tailoring macroscopic materials response [1, 2]. Polymer-ceramic composites are increasingly used for applications, as they usually present higher piezoelectric coefficients and dielectric constant when compared to the matrix polymeric material and higher flexibility, lower density and mechanical losses when compared to the ceramic material [3, 4]. The ceramic-polymer composite properties depend, together with matrix and filler characteristics, on the connectivity, i.e. how the filler and the matrix are interact with each other [5].

Poly(vinylidene fluoride) (PVDF) is a semi-crystalline polymer with an uncommon polymorphism among polymeric materials. PVDF presents four crystalline phases known as α, β, γ and δ, depending of the processing conditions [6]. Typically, the α-phase is obtained by crystallization from the melt and presents a non-polar crystalline structure TGTG'[7]. Also, the α-phase can be obtained from solution cast when the solvent evaporation temperature occurs above 120 ºC [8, 9]. The β-phase shows the highest ferro-, pyro- and piezoelectric properties and is mostly obtained by stretching the α-PVDF at temperatures below 100 ºC and draw ratios between 2 and 5 [8, 9]. Unoriented films exclusively in the β-phase can be also obtained from the crystallization of the PVDF dissolved in different polar solvents (N,N-dimethyl formamide (DMF) or dimethyl acetamide (DMA)) at temperatures below 70 ºC. The resulting material shows high porosity what makes it opaque and fragile [10, 11]. Also, it has been also revealed that PVDF in the β-phase can be also obtained under different manufacturing conditions after the inclusion of specific fillers such as ferrites [12], ionic liquids [13] or zeolites [14], among others.

With respect to the dielectric properties, PVDF presents a crystallization phase dependent high room temperature dielectric constant between 6 and 15 [15], and two main relaxation processes: one at temperatures below -20 ºC, labeled α_a or β and attributed to the amorphous regions and the α or α_c-relaxation at temperatures above 80 ºC and associated with molecular motions within the crystalline fraction [16-18].

Lead zirconate titanate, with chemical formula of $Pb[Zr_xTi_{1-x}]O_3$, $0<x<1$ (PZT), crystallizes in a perovskite structure (ABO_3) [19]. PZT ceramics are widely used in device applications such as micro-mechanical systems, piezoelectric transducers, micro-actuators and pyroelectric sensors, among other [20, 21]. The PZT phase diagram is complex due to existence of a morphotropic phase boundary (MPB) that divides the ferroelectric region into two parts: a tetragonal crystalline phase rich in Ti atoms and a rhombohedral phase region rich in Zr atoms. The MPB occurs in the Zr/Ti = 52 / 48 region and the material is characterized by the highest value of the dielectric constant and the piezoelectric response [22]. Thus, the material in the MPB is widely used in many applications such as sensors [23], transducers [24], energy harvesting [25], among others. Polymer/PZT composites for technological applications raised early attention due to the interesting properties as smart and multifunctional materials [26]. For PVDF/PZT system, it was detected that the piezoelectric effect is mainly due to the ceramic particles, which was supported by mathematical formalisms developed to predict the elastic modulus, dielectric and piezoelectric values of binary polymer/PZT systems [27]. Generally, the high value of the dielectric constant of the ceramic filler allows a higher complex permittivity for the polymer/ceramic composites for moderate volume fractions of PZT filler and present stronger piezoelectric value than in the neat polymer.

The viscoelastic properties of the polymer/PZT composites depend on the ceramic amount, strain and frequency. Generally, polymer/ceramic composites become stiffer and

more brittle with increasing ceramic amount, and exhibit non-linear stress *vs* strain behavior [28].

The effect of filler volume fraction on PVDF/PZT composites with 0-3 connectivity was performed by Zhang et al [29]. The PVDF/PZT composites were prepared by two different shaping processes, hot and cold press It was demonstrated that the piezoelectric and dielectric responses of hot-pressed PVDF/PZT composites are superior to those prepared by cold-pressing methods due to both the formation of β-PVDF and the better coupling of the these materials in the hot-press processing [29] .

The dielectric properties of PVDF/PZT composites are reported in [30] as a function of filler content, and this behavior was interpreted in the light of different theoretical models [31].

The present work, on the other hand, focus on the understanding of the dependence of the dielectric relaxation processes through the Havriliak-Negami formalism as a function of the ceramic amount and size, as well as in relation with the main crystalline phases (α and β) of the PVDF polymer.

In this work, PVDF/PZT composite samples with different PZT concentrations and particle size were produced by solution casting technique in the non-polar and polar phases of PVDF: α and β-phase, respectively. The influence of the PZT amount and particle size on the overall dielectric response of two PVDF matrix (α and β-phase) composites was evaluated, focusing in the different relaxations process detected in the dielectric behavior, which is of critical relevance scientifically and for technological applications. It is to notice that despite being performed for PVDF/PZT composites and also, the results are of general interest for related PVDF/ceramic microcomposites such as the ones based on $BaTiO_3$ [32], Sodium niobate ($NaNbO_3$) [33], or lead-free $_{0.50}[Ba(Zr_{0.2}Ti_{0.8})O_3]_{0.50}(Ba_{0.7}Ca_{0.3})TiO_3$ (BZT-BCT) [34], among others.

2. Dielectric Relaxation Spectroscopy: Theory and Analysis

Dielectric relaxation spectroscopy (DRS) is widely applied to assess molecular motions and structural relaxations present in insulator materials possessing permanent dipolar moments [35].

The complex permittivity:

$$\varepsilon^* = \varepsilon' - i\varepsilon'' \tag{1}$$

can be presented, according to the Debye theory as:

$$\varepsilon^* = \varepsilon_\infty + \frac{\varepsilon_0 - \varepsilon_\infty}{1 + i\omega\tau} \tag{2}$$

where τ is a temperature-dependent relaxation time following an Arrhenius (eq. 3) or a Vogel-Tammann-Fulcher-Hesse (VTFH) (eq. 4) law:

$$\tau = \tau_0 exp\left[\frac{E_{act}}{K_B T}\right] \tag{3}$$

$$\tau = \tau_{0-VTFH} exp\left[\frac{B}{K_B(T - T_0)}\right] \tag{4}$$

where K_B is the Boltzmann constant, E_{act} is the activation energy and T the temperature (eq. 3); and T_0 is the critical temperature at which molecular motions in the material become infinitely slow. B is the activation energy of the relaxation process [36] (eq. 4).

Assuming that the ralaxation process is defined by a superposition of M independent Debye-like processes with a continuous normalized distribution of relaxation times $G(\ln(\tau))$, then:

$$\varepsilon^*(\omega, T) = \varepsilon_\infty + \Delta\varepsilon \int_{-\infty}^{+\infty} \frac{G(\ln \tau))}{1 + i\omega\tau} dln(\tau) \tag{5}$$

with $\Delta\varepsilon = \varepsilon_0 - \varepsilon_\infty$ and the normalization condition $\int_{-\infty}^{+\infty} \frac{G(\ln \tau))}{1 + i\omega\tau} dln(\tau) = 1$. Then, the complex permittivity is given by:

$$\varepsilon'(\omega,T) = \varepsilon_\infty + \Delta\varepsilon \int_{-\infty}^{+\infty} \frac{G(\ln\ \tau))}{1+\omega^2\tau^2} dln(\tau) \quad (6)$$

$$\varepsilon''(\omega,T) = \Delta\varepsilon \int_{-\infty}^{+\infty} \frac{G(\ln\ \tau))}{1+\omega^2\tau^2} dln(\tau) \quad (7)$$

Through these equations, the distribution function can be calculated numerically from the dielectric results.

The complex dielectric permitivitty can be fitted by using Havriliak-Negami (HN) function [37, 38]:

$$\varepsilon^* = \varepsilon_\infty \sum_k \frac{\Delta\varepsilon_k}{[1+(i\omega\tau_k)^{a_k}]^{b_k}} \quad (8)$$

where k is the index over which the relaxation process is assumed and a_k and b_k are fractional parameters ($0 < a_k \leq 1$ and $0 < a_k . b_k \leq 1$) describing, the symmetric and asymmetric broadnening of the complex dielectric function [39], respectively.

3. Experimental details

3.1.Samples preparation

PVDF/PZT composite films were obtained from PVDF polymer and PZT ceramic particles with three different particles sizes (0.84, 1.68 and 2.35 μm) following the method described elsewhere [10, 31]. The used solvent was dymethylacetamide (DMA) and the polymer/solvent ratio 20/80 wt%, The thickness of the composites films is ~30 μm.

After the stirring process and polymer dissolution, the solution was spread on a glass plate through bar coating and, in order to allow the crystallization of the β-PVDF phase, the solvent was evaporated at 65 ºC for 1 h [40] and then at 80 ºC for 12 h to remove any trace of DMA. α- PVDF was obtained after heating above the melting temperature of the composites at 220 ºC for 10 min and cooling down to 25 ºC [40].

The amount of ceramic filler ($\emptyset = 1.68\,\mu m$) is in the range between 10 to 40 % (in volume) for the α-phase matrix composites. PZT percentages until 40 wt.% result in PVDF-PZT composites in which the 0-3 connectivity is preserved. α-phase matrix composites with 20% of ceramic filler content with diameter 0.84, 1.68 and 2.35 μm, were also prepared. The β-phase matrix composites were prepared with 30 and 40% of PZT particles with diameter 1.68 μm.

3.2.Dielectric characterization

Dielectric measurements were performed by impedance spectroscopy (Alpha-S, Quatro Cryosystem from Novocontrol GmbH). In order to obtain a parallel plate capacitor, circular gold electrodes with 5 mm radius were deposited by sputtering on both sides of sample. The sample cell was mounted in a cryostat (BDS 1100) from a liquid nitrogen *deward*. The complex dielectric permittivity $\varepsilon^* = \varepsilon' - i\varepsilon''$ was calculated as a function

of frequency (10^{-1} – 10^{7} Hz) and isothermal temperatures ramps from −120 ºC to 150 ºC (thermal stability: 0.1 ºC) and a step of 5 ºC.

4. Results and discussions

4.1. α-phase PVDF matrix

The influence of the processing conditions on the distribution of the ceramic fillers in the PVDF matrix was evaluated in previous works, and it was detected that PZT particles are randomly distributed within the polymeric matrix without aggregates in both α- and β-phase PVDF with a 0-3 connectivity [10, 31, 41]. The cross-section images for the composites with higher ceramic content are shown in Figure S1 (supplementary information), in which a good distribution of the ceramic particles in the polymer matrix can be observed, regardless of the ceramic particle size. With respect to the polymer microstructure, the large spherulites of α-PVDF disappear with increasing ceramic content, whereas in composites materials crystallized in the β-phase, the increase filler amount reduces the polymer porosity [11, 41].

The crystalline phase of the PVDF/PZT composites is not affected by the PZT content and average size [41].

Figure 1 shows the frequency and temperature dependence of the dielectric response for α-PVDF and corresponding composite for 30% PZT. It is observed an increase of the dielectric constant with increasing PZT amount, in agreement with previous reports [10, 31]. Figure 1 presents the low-temperature β-relaxation characteristic of the neat PVDF polymer, assigned to the local micro-Brownian movements of molecular segments in the non-crystalline region at temperatures below the glass temperature (T_g) of the polymer[16, 17]. Therefore, this process in the amorphous phase is induced by cooperative segmental motions [42].

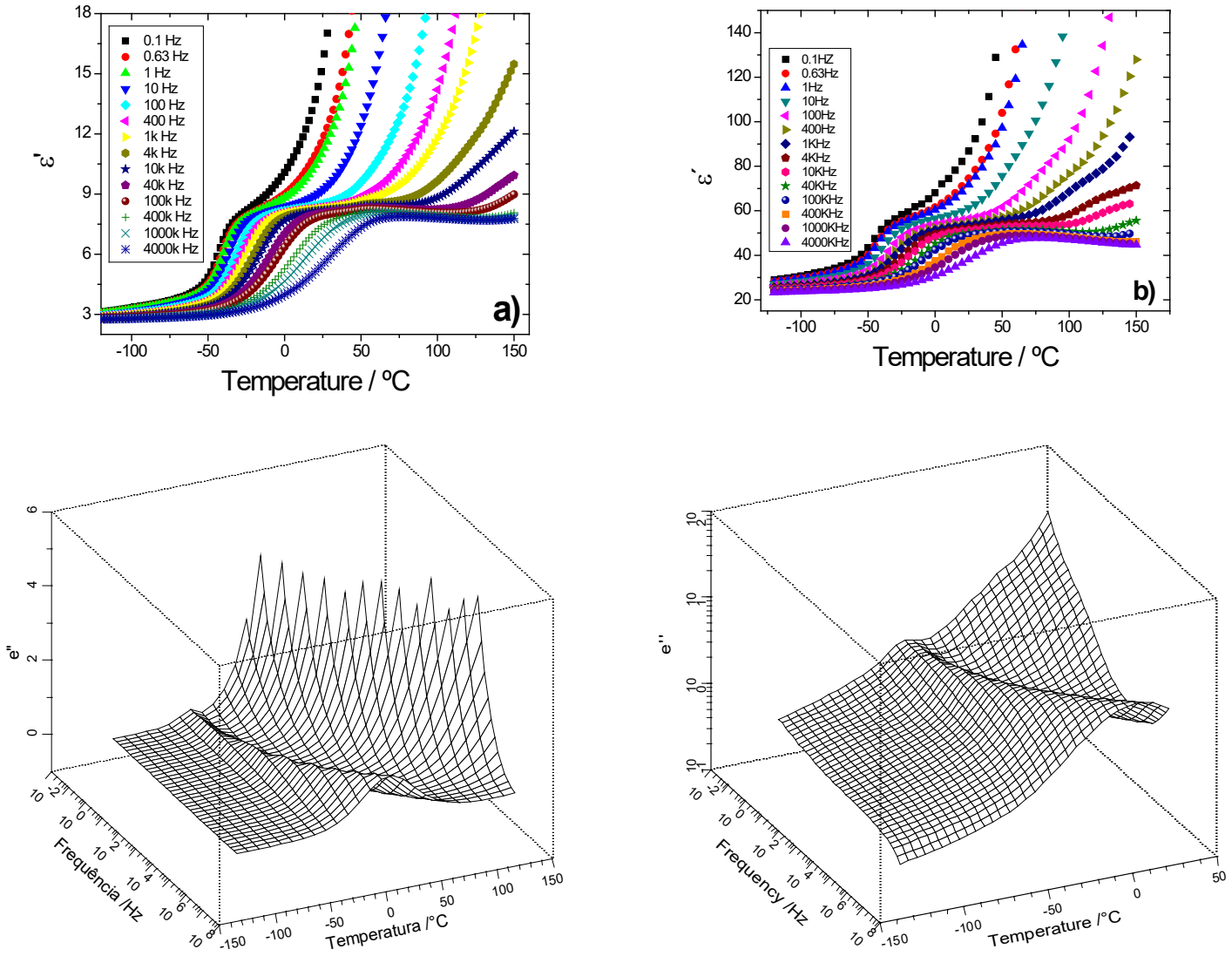

Figure 1 – Complex dielectric permittivity, ε′ and ε′′, as a function of frequency and temperature for α-PVDF a) and c) and α-phase PVDF/PZT composites b) and d) with 30 % PZT filler amount with average size of $\emptyset = \mathbf{1.68}$ μm.

The α_c-relaxation of the PVDF matrix is proposed to appear at temperatures above 80 ºC [15]. This relaxation is related with molecular motions within the crystalline fraction of the material. However, instead of a clear observation of the α_c-relaxation, it is detected that the dielectric constant increases, related to the high conductivity due to interface effects, is observed for all the composites, hiding the α_c-relaxation process (Figure 1).

In experimental studies on polymer dynamics with broadband dielectric spectroscopy, the experimental variation of the complex permittivity, ε^*, as a function of the frequency (ω) and temperature (T) is commonly described assuming a distribution function of relaxation times, contributing to each relaxation process. Using a general approach, the exponential decay function is used together with an empirical distribution function, $G(\ln(\tau))$, which describes the superposition of exponentially damped processes. The parameters that describe this function are obtained by the best fit of the experimental results [43].

Several empiric mathematical expressions have been used to explain the variation of the $\varepsilon^*(\omega)$ in glass-forming polymeric materials, such as the Debye [39], Cole-Cole [44], Cole-Davinson [45] and Havriliack-Negami [38] relaxation functions. Through these equations, the distribution of relaxation times is found analytically.

In this work, the dielectric relaxation has been described empirically by the Havriliack-Negami (HN) equation 8, as it is the most adequate for the description of semicrystalline polymers (see in supplementary information, Figure S2 with fits by HN equation). The HN formalism allows the study of the dielectric behavior of the PVDF/PZT composites and, comparing the data obtained with the neat polymer, to evaluate the filler effect on the low temperature relaxation.

Figure 2 shows the relaxation strength ($\Delta\varepsilon$) as a function of temperature for the β-relaxation process for the α-phase matrix.

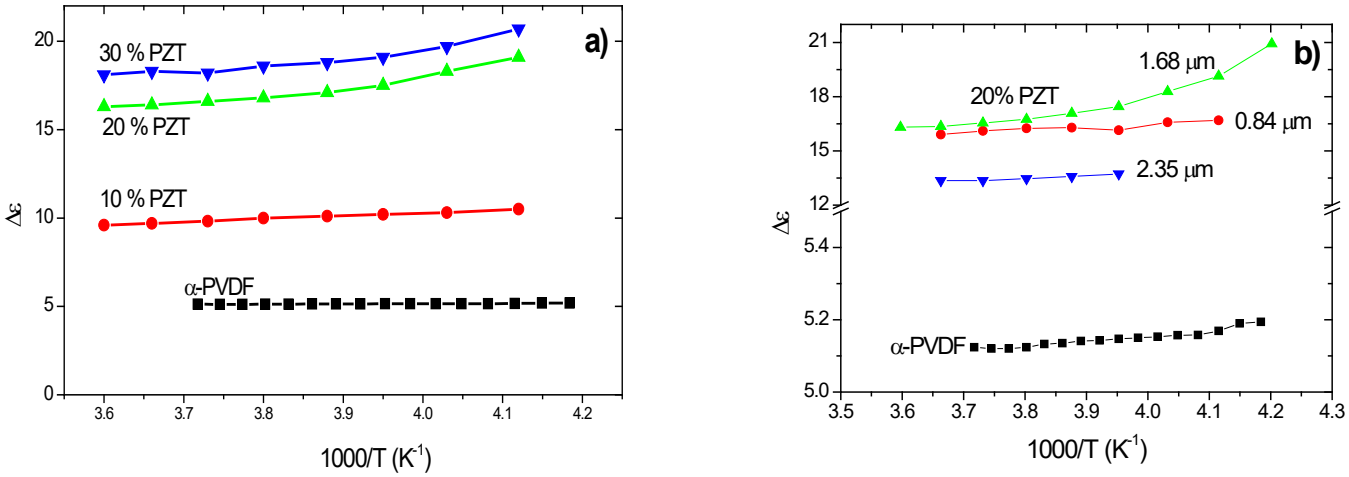

Figure 2 – Relaxation strength for the α-phase PVDF/PZT composites: a) α-phase PVDF sample with different PZT ($\emptyset = 1.68\,\mu m$) contents and b) samples with 20% PZT ceramic amount and different average particle size.

It is observed that Δε increases with increasing PZT filler amount in the polymer matrix for a given filler average particle size (figure 2a). Also, identical values are obtained for a given PZT amount, being nearly independent of the PZT average size. These facts demonstrate that the dielectric strength of the relaxation process is affected by the PZT filler amount and size (for the particle sizes under study).

The slight decrease of the dielectric strength for the 20% PZT sample with PZT filler average size of 2.35 μm is to be ascribed to the presence of clusters for higher filler size composites [10, 31]. For higher electroactive PZT contents (20 % or higher) in the PVDF/PZT composite samples, the spherulitic structure is destroyed and the polymeric material only clumps in the free space between the ceramic particles [10, 31]. The crystallization kinetics of the α-PVDF polymer is attributed to spherulitic growth with heterogeneous nucleation where the spherulite sizes varies from 10 to 100 μm, depending on the crystallization temperature [10]. The presence of the PZT microparticles interfere both in the spherulites growth kinetic and the nucleation process [10, 46]. For low amounts of PZT microparticles, mainly the nucleation process in PVDF/PZT composites

will be affected. The size of the PVDF spherulites is smaller in the PVDF/PZT composites with the lowest particles and, in both cases, smaller than in the neat PVDF polymer. It was verified that the number of crystallization nuclei is greater for the PVDF/PZT composite containing 0.84 μm particles, where a more effective nucleation of the PVDF polymer for small particles is detected. In addition, the change in the crystallization kinetics disturbs the degree of crystallinity of the PVDF polymer. For higher concentrations above 20wt.% of PZT, the PZT microparticles prevent the growth of spherulites and, therefore, avoid the formation of the PVDF characteristic spherulitic microstructure [31]. The polymer phase in these composites is dispersed over very small domains, which restrict the growth of crystals. A fraction of the polymer chains is restricted between PZT microparticles and within the aggregates. The ceramic particle size plays an important role in the aggregate's formation, in particular for PVDF/PZT composites samples with filler concentrations of 20% or larger. Figure 2 shows for larger microparticle diameters, the aggregates show higher dimensions, resulting in a decrease of the dielectric strength of α-PVDF/PZT composites.

The changes of the shape parameter (a_k) with filler content and average size is represented in Figure 3.

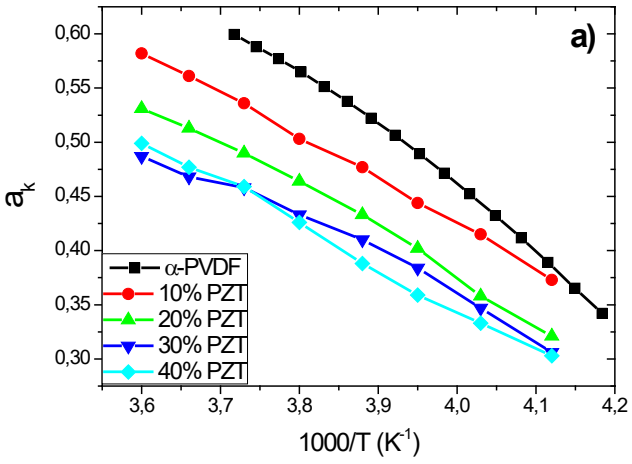

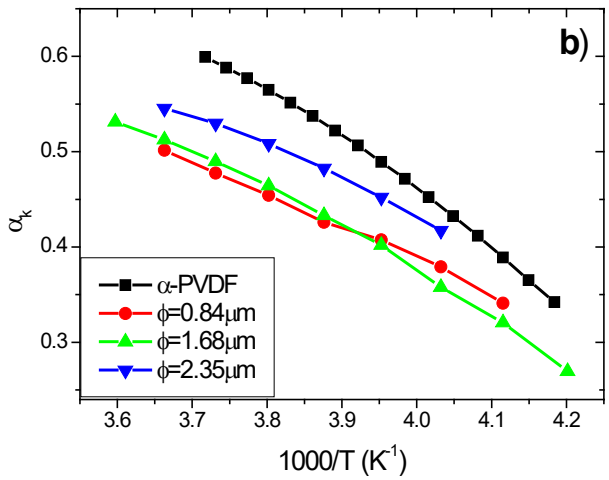

Figure 3 – a_k parameter evolution for the α-phase PVDF/PZT composites: a) α-phase PVDF samples with different PZT contents ($\emptyset = 1.68\ \mu m$) and b) samples with different average particle size and 20 wt.% PZT ceramic.

The evolution of the a_k parameter of the HN model displays a decrease with increasing ceramic filler content (Figure 3a). Also, a decrease of the a_k parameter is observed especially for the composite sample with smaller average particle size ($\emptyset = 0.84\ \mu m$) (Figure 3b). This behavior is to be ascribed to variations in the polymer nucleation kinetics due to the presence of the PZT microparticles in the PVDF matrix. Typically, the polymeric chains are constrained between the PZT aggregates that are greater for the higher ceramic particles [10, 46]. In fact, it was previously discovered that the presence of PZT microparticles in PVDF/PZT composites decreases the degree of crystalline phase [31, 41], which explains the evolution of the α_k parameter. The evolution of the b_k parameter with increasing PZT content and average particle size is represented in Figure 4.

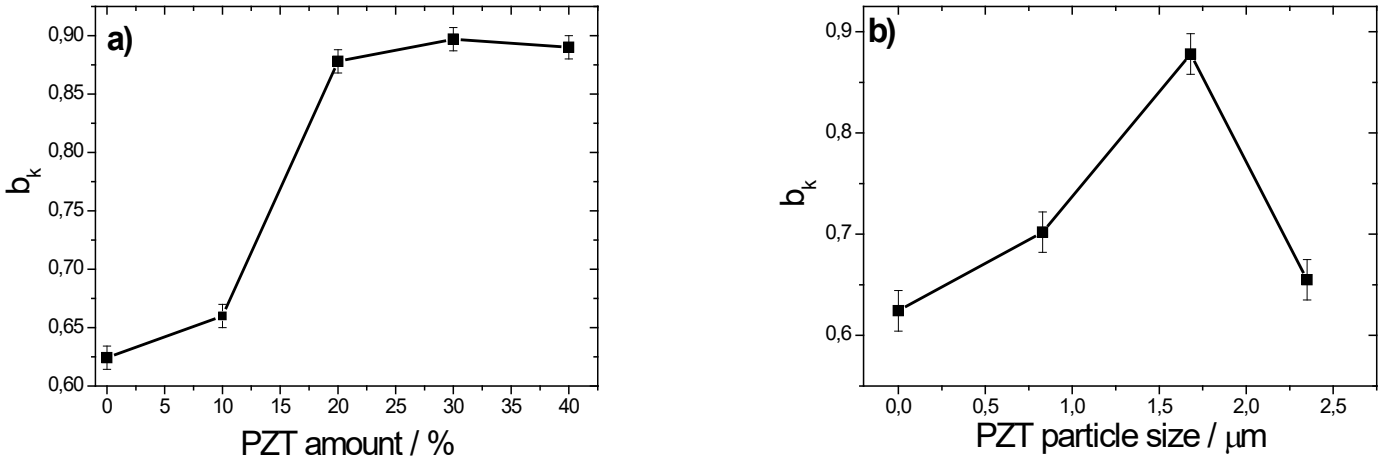

Figure 4 – of the b_k HN fitting parameter for the α-phase PVDF/PZT composites: a) with different PZT amount ($\emptyset = 1.68\ \mu m$) and b) samples with different average particle size and 20wt.% of PZT ceramic amount.

The evolution of the b_k parameter of the HN model reveals an increase with the amount of PZT microparticles until a maximum is reached for the sample with 30 % PZT content, remaining stable for further increasing PZT microparticle amount (Figure 4a). Moreover, an increase of the b_k is also detected for PVDF/PZT composites with the same amount of PZT filler and different average particle size until $\emptyset = 1.68\,\mu m$, decreasing for the sample with the highest average size ($\emptyset = 2.35\,\mu m$) (Figure 4b).

The obtained results prove that the relaxation process shows a wide distribution of relaxation times and that the profile of the process becomes more symmetric for the samples with higher PZT filler content for a given particle size. In addition, the symmetry of the relaxation process is strongly dependent on the particle size, with the symmetry of the process increasing with increasing particle size until a maximum is reached for the sample with $\emptyset = 1.68\,\mu m$.

As stated above, this behavior is probably associated to the nucleation kinetics of PVDF, hampered by the presence of PZT particles present in the matrix. Especially for higher concentrations (20% PZT or higher) the presence of electroactive ceramic filler hamper the crystallites from growing freely, preventing the formation the characteristic crystallization structure of the PVDF polymer matrix. The polymeric chains are then constrained between the PZT aggregates that are larger for the larger ceramic particles [10, 46].

The overall behavior of this relaxation process correlates well with the decrease of the degree of crystallinity for PZT amount [31, 41].

The relaxation time (τ_0) with temperature for the β-relaxation follows the dependence of the Vogel-Fulcher-Tammann-Hesse law (equation 3). Figure 5 shows the relaxation time behavior for the β-relaxation, for samples with different ceramic content and a given filler

size ($\emptyset = 1.68\,\mu m$) and for a given concentration (20% PZT) and different PZT microparticle average sizes.

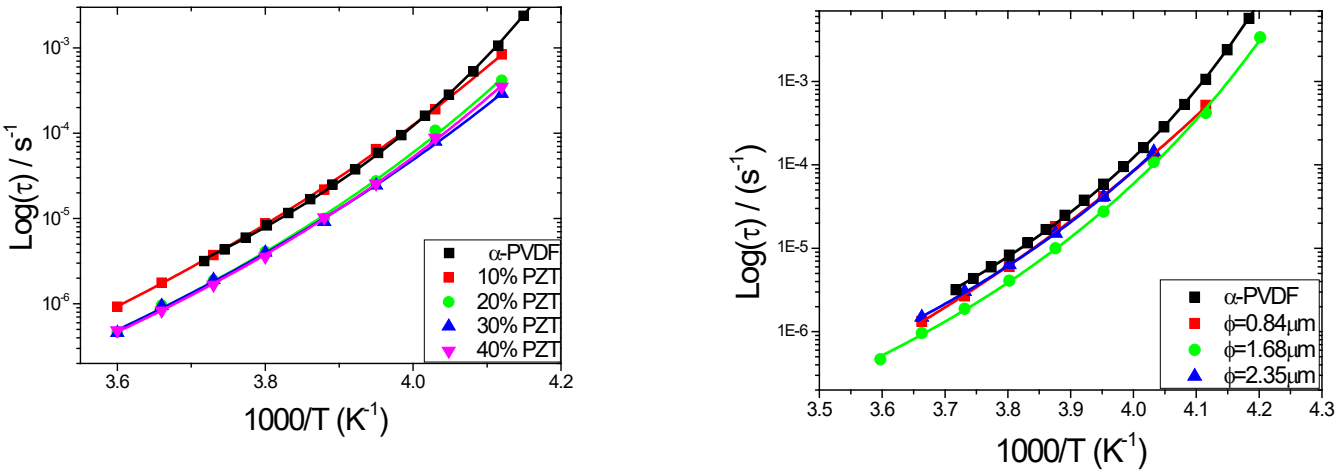

Figure 5 – a) Relaxation time dependence with temperature and corresponding fitting with the Vogel-Fulcher-Tammann-Hesse law for the α-phase PVDF/PZT composites ($\emptyset = 1.68$ μm) and b) for different average sizes.

Table 1 shows the parameters for the PVDF/PZT composites with different average particle size and the same PZT amount (20%) found in the VTFH fitting of the β-relaxation. A decrease of τ_0 is observed for the composites when compared to the neat α-PVDF matrix and the same behaviour is found for the T_0 parameter. It is observed that *B* parameter increases with the increase of the ceramic particle amount, especially for the sample with $\emptyset = 0.84\,\mu m$ (Table 1).

Table 1 – Evolution of the VTFH fitting parameters and fragility (m) for the α-phase PVDF/PZT samples with different filler content (($\emptyset = 1.68\,\mu m$) and different average particles sizes.

α-phase matrix (ϕ = 1.68 μm)	**$\tau_{0\text{-VTFH}}$ (s^{-1})**	***B* (eV)**	**T_0 (K)**	**m**
0%	5.59×10^{-10}	0.059	204	98.1
10% PZT	7.05×10^{-13}	0.131	170	65.7

20% PZT	4.62×10^{-12}	0.095	183	81.3
30% PZT	1.01×10^{-12}	0.121	171	68.9
40% PZT	3.71×10^{-12}	0.098	181	79.5
20% PZT ϕ =0.84 μm	4.59×10^{-13}	0.135	168	65.1
20% PZT ϕ =2.35 μm	7.53×10^{-11}	0.068	193	94.9

Based on the representation of the relaxation times against glass transition temperature, a method was to classify glass-forming liquids from "strong" to "fragile" [47, 48]. Considering this concept, the fragility parameter (m), related to the amorphous phase of PVDF, is assessed through the HN fitting parameters and calculated by:

$$m = \frac{{}^{B}/_{K_B T_g}}{(\ln 10)\left(1-{}^{T_0}/_{T_g}\right)^2} \quad (9)$$

The dynamic fragility characterized by the velocity with which a liquid's dynamic properties (relaxation time, viscosity, …) varies as the glass transition temperature (T_g) is reached. 'Fragile' systems are characterized by m > 50 and 'strong' ones, close to Arrhenius behavior, show m values lower than 30.

The values of the fragility parameter, included in Table 1, show that the PVDF/PZT composites present a fragile behavior, also observed in Fig. 5, with PVDF showing a fragility parameter ~100: The PZT microparticles incorporation results in a substantial decrease in fragility (more 'strong' behavior). Moreover, there is a high dependence on fragility as a function of particle size. Samples with 20% PZT and minimum diameter ($\emptyset = 0.84\ \mu m$) show the lowest m value (strongest behavior), increasing the fragility as particle size does. These results suggest that the particle-matrix interaction induce heterogeneity in the polymer matrix (which increases with the content of particles), leading to a more 'strong' behavior [49].

As stated before, the β-relaxation is related to cooperative segmental motions of molecular segments in non-crystalline regions. The values found for the HN fitting parameters for the β-relaxation suggests that this process, in addition to being associated to the movements of the PVDF amorphous phase, contains a contribution of the polymer crystalline part and from the interface between the ceramic microparticles and the polymer. An increase of the PZT amount restrains the chain movement and the contribution of the molecular dynamics of relaxation can be impaired by the PVDF crystalline phase [50] and from the PZT particles present in the composite sample.

4.2. β-phase PVDF matrix

Analysis of the complex permittivity values were also obtained for β-PVDF/PZT composites, in order to evaluate the polymer matrix effect on the dielectric response. The results are similar to the ones presented in Figure 1 for α-PVDF/PZT composites and are summarized in Figure S3 for the complex permittivity of neat β-PVDF and the β-PVDF/PZT composites.

Regardless of the polymer phases (α- and β-phase) and for PVDF/PZT composites, the addition of PZT microparticles in the PVDF matrix increases the dielectric constant (Figure 1 and S3). Figure S3 shows that the room temperature real part of the permittivity increases more than 10 times for the composite with the highest amount of the PZT microparticles ($\varepsilon' \approx 810$) when compared to neat PVDF polymer ($\varepsilon' = 7$ and 16 , for α and β-PVDF, respectively, at 25 ºC and 1 kHz [10, 31].

The size of the PZT microparticles is also relevant to the final ε' values of the PVDF/PZT composite, the ε'values being slightly larger for the smaller PZT grain sizes. It can be detected that the PZT fillers in the PVDF/PZT composites are the main contribution to the value of the dielectric constant [10, 31]. A detailed theoretical and experimental

description of the filler dependent dielectric behaviour of the composites has been described elsewhere [10, 31].

Likewise, the dielectric relaxation behavior of β-phase PVDF/PZT composites was studied according to the HN mathematical formalism (equation 8). The behavior of the relaxation strength (Δε) for the β-relaxation process for the β-PVDF matrix ($\emptyset = 1.68\ \mu m$) with temperature is represented in Figure 6a.

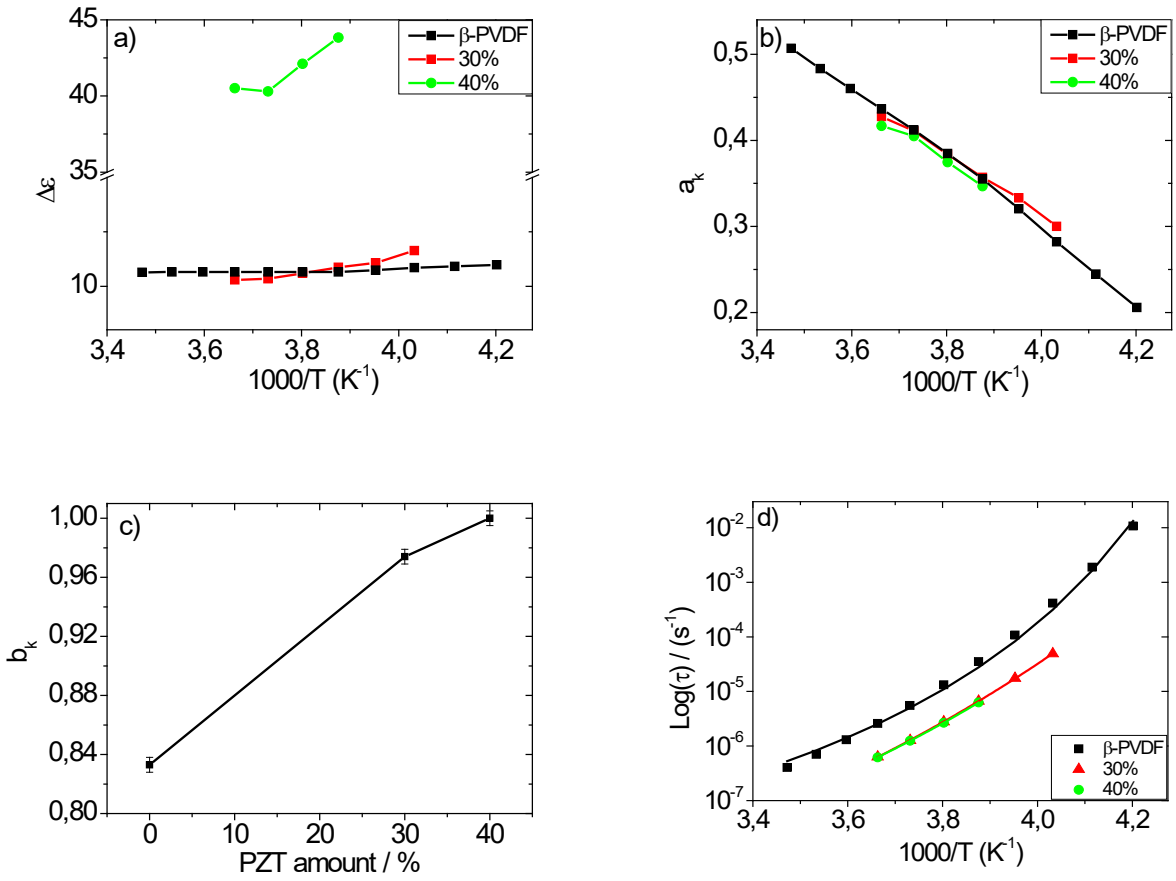

Figure 6 – a) Relaxation strength for the β-phase PVDF/PZT composites with different PZT amounts ($\emptyset = 1.68\ \mu m$). b) Evolution of the a_k and c) evolution of the b_k: determined by the HN for β-phase PVDF and β-phase PVDF/PZT composites. d) Temperature dependence of the relaxation time and corresponding fit with Vogel-Fulcher-Tammann-Hesse law for the β-phase PVDF/PZT composites with different PZT contents

Figure 6a) shows a significant increase in Δε when the PZT filler quantity in the polymer matrix increases from 30 to 40% in the PVDT/PZT composites with the same particle average size ($\emptyset = 1.68\,\mu m$). Also, it is observed that the dielectric strength is strongly influenced by the PZT filler amount present in the composite. The inclusion of the PZT microparticles reduces the crystallinity and polymer crystallization (*in β-phase*) occurs in a confined space which can induce inability of the polymeric amorphous phase dipoles to relax in all spatial directions.

It has been reported previously [10, 31] that the crystalline structure is lost and the polymer material agglomerates on the free space between the ceramic particles when the PZT microparticles present in the composite are equal or higher than 20%. The crystallization kinetics of the β-PVDF polymer is characterized by heterogeneous nucleation with spherulitic growth [11]. Nevertheless, the addition of the ceramic particles hampers both in the growth kinetic of the crystallites and in the nucleation process [31, 41]. For low concentration of ceramic microparticles, mainly the nucleation process will be affected. In addition, a higher electroactive ceramic concentration hinders the crystallites growth and therefore prevents the formation of the characteristic microstructure of the polymer [31, 41]. In fact, the polymer phase in the PVDF/PZT composites is spread over very small domains, where crystal growth is limited. A fraction of the PVDF polymer chains is confined between PZT micro particles, also within the aggregates.

Changes of a_k and b_k parameters with different filler contents obtained from the HN fitting are represented in Figure 6b and c. Figure 6b shows that the evolution of the a_k parameter does not present significant variations with increasing ceramic filler in the PVDF/PZT composites. By contrast, an increase of the b_k parameter is observed with increasing PZT filler amount in the PVDF/PZT composites. These results show that the

β-relaxation process is broad and the shape of the process becomes more symmetrical as the amount PZT filler increases (Figure 6c). As stated above, this behavior indicates a disruption in the PVDF nucleation kinetics originated by the PZT microparticles in the polymer matrix.

Figure 6d shows the dependence of the β-relaxation time distribution (τ_{HN}) as a function of temperature follows the Vogel-Fulcher-Tammann-Hesse law (equation 3) for the β-relaxation process in the β-PVDF/PZT composites.

The parameters obtained for the VTFH fitting are represented in Table 2. For the PVDF/PZT composites, the τ_0 decreases when compared to the β-PVDF matrix; the same behaviour is found for the T_0 parameter. Finally, an increase in the B parameter is observed, which increases with the ceramic particle content in the composite (Table 2).

Table 2 – Evolution of the VTFH fitting parameters for the β-PVDF/PZT samples with different amounts of PZT ($\emptyset = 1.68\ \mu m$).

β-PVDF matrix ($\emptyset = 1.68\ \mu m$)	**$\tau_{0\text{-VTFH}}$ (s^{-1})**	**B (eV)**	**T_0 (K)**	**m**
0	$2.73*10^{-10}$	0.068	200	89.6
30% PZT	$9.36*10^{-14}$	0.157	158	60.1
40% PZT	$4.36*10^{-14}$	0.131	166	74.7

Table 2 shows that the fragility parameter, *m*, behavior is similar to that of *α-phase* composites. The inclusion of PZT filler, leading to a more heterogeneous microstructure, results in a more "strong" behavior when compared to the pure β-PVDF.

The NH fitting and fragility parameters obtained from the β-phase PVDF matrix composites, in an analogous manner as the α-phase composites, suggest that the dynamics of this relaxation process is associated to motions in the PVDF amorphous phase with the

influence of the crystalline phase [50], being also contributions from the polymer-filler interfaces.

Conclusions

PVDF/PZT composite materials with PZT amounts (10 to 40 wt.%) and particle size were prepared in the non-polar and polar phases of the PVDF: α– and β-phase, respectively. The dielectric spectrum displays that the low-temperature β-relaxation of the amorphous phase in PVDF polymer, related to the cooperative segmental motion, is strongly affected by the presence of PZT filler, in both α– and β- polymer matrix. The fitting parameters determined by the HN model, together with the 'fragility' parameter indicate that the PZT particles induce heterogeneity in the polymer matrix. The relaxation dynamic reveals that changes in the process are related to the motions in the amorphous phase of PVDF polymer with the influence of the crystalline phase, strongly affected by the PZT filler, and the interface between the polymer chains and PZT particles.

Acknowledgments

The authors thank the FCT (Fundação para a Ciência e Tecnologia) for financial support under the framework of Strategic Funding grants UID/FIS/04650/2019, and UID/EEA/04436/2019; and project PTDC/FIS-MAC/28157/2017. The author also thanks the FCT for financial support under grant SFRH/BPD/112547/2015 (C.M.C.). Financial support from the Spanish State Research Agency (AEI) and the European Regional Development Fund (ERFD) through the project PID2019-106099RB-C43 / AEI / 10.13039/501100011033 and from the Basque Government Industry and Education Departments under the ELKARTEK, HAZITEK and PIBA (PIBA-2018-06) programs, respectively, are acknowledged. CIBER-BBN is an initiative funded by the VI National

R&D&I Plan 2008–2011, Iniciativa Ingenio 2010, Consolider Program. CIBER Actions are financed by the Instituto de Salud Carlos III with assistance from the European Regional Development Fund. The authors thank Prof. R. Gregorio Filho, University Federal of S. Carlos, Brazil, for providing the ceramic particles.

References

[1] Groover MP. Fundamental of Modern Manufacturing. New York: John Wiley & Sons, Inc; 2002.

[2] Nelson JK. Dielectric Polymer Nanocomposites: Springer US; 2009.

[3] Dias CJ, Das-Gupta DK. Inorganic ceramic/polymer ferroelectric composite electrets. Dielectrics and Electrical Insulation, IEEE Transactions on. 1996;3(5):706-34.

[4] Dias CJ, Wenger MP, Kaminorz Y, Hopfner U, Das-Gupta DK. Electro-active properties of intelligent ferroelectric ceramic/polymer composite sensors. Electrets, 1994 (ISE 8), 8th International Symposium on1994. p. 589-93.

[5] Newnham RE, Skinner DP, Cross LE. Connectivity and piezoelectric-pyroelectric composites. Materials Research Bulletin. 1978;13(5):525-36.

[6] Nalwa HS. Ferroelectric polymers: chemistry, physics and applications. New York: Marcel Dekker; 1995.

[7] Martins P, Lopes AC, Lanceros-Mendez S. Electroactive phases of poly(vinylidene fluoride): Determination, processing and applications. Progress in Polymer Science. 2014;39(4):683-706.

[8] V. Sencadas, V. M. Moreira, S. Lanceros-Mendez, Pouzada AS, Jr. RG. α- to β-Transformation on PVDF Films Obtained by Uniaxial Stretch. Materials Science Forum. 2006;514-516:872-6.

[9] Sencadas V, Gregorio R, Lanceros-Méndez S. α to β Phase Transformation and Microestructural Changes of PVDF Films Induced by Uniaxial Stretch. Journal of Macromolecular Science, Part B: Physics. 2009;48(3):514 - 25.

[10] Sencadas V, Costa C, Gómez Ribelles J, Lanceros-Mendez S. Isothermal crystallization kinetics of poly(vinylidene fluoride) in the α-phase in the scope of the Avrami equation. Journal of Materials Science. 2010;45(5):1328-35.

[11] Sencadas V, Gregorio Filho R, Lanceros-Mendez S. Processing and characterization of a novel nonporous poly(vinilidene fluoride) films in the β phase. Journal of Non-Crystalline Solids. 2006;352(21-22):2226-9.
[12] Martins P, Caparros C, Gonçalves R, Martins PM, Benelmekki M, Botelho G, et al. Role of Nanoparticle Surface Charge on the Nucleation of the Electroactive β-Poly(vinylidene fluoride) Nanocomposites for Sensor and Actuator Applications. The Journal of Physical Chemistry C. 2012;116(29):15790-4.
[13] Correia DM, Costa CM, Lizundia E, Sabater i Serra R, Gómez-Tejedor JA, Biosca LT, et al. Influence of Cation and Anion Type on the Formation of the Electroactive β-Phase and Thermal and Dynamic Mechanical Properties of Poly(vinylidene fluoride)/Ionic Liquids Blends. The Journal of Physical Chemistry C. 2019;123(45):27917-26.
[14] Lopes AC, Caparros C, Ferdov S, Lanceros-Mendez S. Influence of zeolite structure and chemistry on the electrical response and crystallization phase of poly(vinylidene fluoride). Journal of Materials Science. 2013;48(5):2199-206.
[15] Sencadas V, Lanceros-Méndez S, Sabater i Serra R, Andrio Balado A, Gómez Ribelles JL. Relaxation dynamics of poly(vinylidene fluoride) studied by dynamical mechanical measurements and dielectric spectroscopy. The European Physical Journal E. 2012;35(5):41.
[16] Boyd RH. Relaxation processes in crystalline polymers: experimental behaviour -- a review. Polymer. 1985;26(3):323-47.
[17] Boyd RH. Relaxation processes in crystalline polymers: molecular interpretation -- a review. Polymer. 1985;26(8):1123-33.
[18] Tian L-y, Huang X-b, Tang X-z. Study on morphology behavior of PVDF-based electrolytes. Journal of Applied Polymer Science. 2004;92(6):3839-42.
[19] Wong GHL, Chua BW, Li L, Lai MO. Processing of thermally stable doped perovskite PZT ceramics. Journal of Materials Processing Technology. 2001;113(1-3):450-5.
[20] Scott JF. New developments on FRAMs: [3D] structures and all-perovskite FETs. Materials Science and Engineering B. 2005;120(1-3):6-12.
[21] Haertling GH. Ferroelectric Ceramics: History and Technology. Journal of the American Ceramic Society. 1999;82(4):797-818.
[22] Wu A, et al. Domain populations in lead zirconate titanate thin films of different compositions via piezoresponse force microscopy. Nanotechnology. 2005;16(11):2587.

[23] Payo I, Hale JM. Sensitivity analysis of piezoelectric paint sensors made up of PZT ceramic powder and water-based acrylic polymer. Sensors and Actuators A: Physical. 2011;168(1):77-89.
[24] Zhou QF, Chan HLW, Choy CL. PZT ceramic/ceramic 0–3 nanocomposite films for ultrasonic transducer applications. Thin Solid Films. 2000;375(1):95-9.
[25] Zhang Y, Bao Y, Zhang D, Bowen CR. Porous PZT Ceramics with Aligned Pore Channels for Energy Harvesting Applications. Journal of the American Ceramic Society. 2015;98(10):2980-3.
[26] Furukawa T, Ishida K, Fukada E. Piezoelectric properties in the composite systems of polymers and PZT ceramics. Journal of Applied Physics. 1979;50(7):4904-12.
[27] Yamada T, Ueda T, Kitayama T. Piezoelectricity of a high-content lead zirconate titanate/polymer composite. Journal of Applied Physics. 1982;53(6):4328-32.
[28] Marra SP, Ramesh KT, Douglas AS. The mechanical properties of lead-titanate/polymer 0-3 composites. Composites Science and Technology. 1999;59(14):2163-73.
[29] Zhang D-Q, et al. Structural and Electrical Properties of PZT/PVDF Piezoelectric Nanocomposites Prepared by Cold-Press and Hot-Press Routes. Chinese Physics Letters. 2008;25(12):4410.
[30] Jain A, K. J. P, Sharma AK, Jain A, P.N R. Dielectric and piezoelectric properties of PVDF/PZT composites: A review. Polymer Engineering & Science. 2015;55(7):1589-616.
[31] Firmino Mendes S, Costa C, Sencadas V, Serrado Nunes J, Costa P, Gregorio R, et al. Effect of the ceramic grain size and concentration on the dynamical mechanical and dielectric behavior of poly(vinilidene fluoride)/Pb($Zr_{0.53}Ti_{0.47}O_3$) composites. Applied Physics A: Materials Science & Processing. 2009;96(4):899-908.
[32] Wang Y, Yao M, Ma R, Yuan Q, Yang D, Cui B, et al. Design strategy of barium titanate/polyvinylidene fluoride-based nanocomposite films for high energy storage. Journal of Materials Chemistry A. 2020;8(3):884-917.
[33] Alexandre M, Bessaguet C, David C, Dantras E, Lacabanne C. Piezoelectric properties of polymer/lead-free ceramic composites. Phase Transitions. 2016;89(7-8):708-16.
[34] Riquelme SA, Ramam K. Dielectric and piezoelectric properties of lead free BZT-BCT/PVDF flexible composites for electronic applications. Materials Research Express. 2019;6(11):116331.

[35] N. G. McCrum, B. E. Read, Williams G. Anelastic and dielectric effects in polymeric solids. New York: John Wiley & Sons Ltd; 1967.
[36] V. Sencadas, C. M. Costa, V. M. Moreira, J. Monteiro, S. K. Mendiratta, J. F. Mano, et al. Poling of β-poly(vinylidene fluoride): dielectric and IR spectroscopy studies e-Polymers. 2005;002:1-12.
[37] S. Havriliack, Negami S. A complex plane representation of the dielectric and mechanical relaxation processes in some polymers. Polymer. 1967;8:161-210.
[38] Havriliak S, Negami S. A complex plane analysis of alpha-dispersions in some polymer systems. Journal of Polymer Science Part C: Polymer Symposia. 1966;14(1):99-117.
[39] F. Kremer, Schönhals A. Broadband Dielectric Spectroscopy. New York: Springer; 2002.
[40] Ribeiro C, Costa CM, Correia DM, Nunes-Pereira J, Oliveira J, Martins P, et al. Electroactive poly(vinylidene fluoride)-based structures for advanced applications. Nature Protocols. 2018;13(4):681-704.
[41] Costa CM, Firmino Mendes S, Sencadas V, Ferreira A, Gregorio Jr R, Gómez Ribelles JL, et al. Influence of processing parameters on the polymer phase, microstructure and macroscopic properties of poly(vinilidene fluoride)/Pb(Zr0.53Ti0.47)O3 composites. Journal of Non-Crystalline Solids. 2010;356(41-42):2127-33.
[42] Lanceros-Mendez S, Moreira MV, Mano JF, Schmidt VH, Bohannan G. Dielectric Behavior in an Oriented b-PVDF Film and Chain Reorientation Upon Transverse Mechanical Deformation. Ferroelectrics. 2002;273(1):15 - 20.
[43] Bello A, Laredo E, Grimau M. Distribution of relaxation times from dielectric spectroscopy using Monte Carlo simulated annealing: Application to alpha -PVDF. Physical Review B. 1999;60(18):12764.
[44] Cole KS, Cole RH. Dispersion and Absorption in Dielectrics I. Alternating Current Characteristics. The Journal of Chemical Physics. 1941;9(4):341-51.
[45] Davidson DW, Cole RH. Dielectric Relaxation in Glycerol, Propylene Glycol, and n-Propanol. The Journal of Chemical Physics. 1951;19(12):1484-90.
[46] Silva MP, Sencadas V, Botelho G, Machado AV, Rolo AG, Rocha JG, et al. α- and γ-PVDF: Crystallization kinetics, microstructural variations and thermal behaviour. Materials Chemistry and Physics. 2010;122(1):87-92.

[47] Angell CA, Moynihan CT, Hemmati M. Strong and superstrong liquids, and an approach to the perfect glass state via phase transition. Journal of Non-Crystalline Solids. 2000;274(1-3):319-31.
[48] Angell CA. Relaxation in liquids, polymers and plastic crystals -- strong/fragile patterns and problems. Journal of Non-Crystalline Solids. 1991;131-133(Part 1):13-31.
[49] Kwon S-C, Adachi T. Strength and fracture toughness of nano and micron-silica particles bidispersed epoxy composites: evaluated by fragility parameter. Journal of Materials Science. 2007;42(14):5516-23.
[50] Harnischfeger P, Jungnickel B-J. Features and origin of the dynamic and the nonlinear piezoelectricity in poly (vinylidene fluoride). Ferroelectrics. 1990;109(1):279 - 84.